# MODULATION OF MACROPHAGE PHENOTYPE THROUGH CONTROLLED RELEASE OF INTERLEUKIN-4 FROM GELATINE COATINGS ON TITANIUM SURFACES

C.L. Yang[1,2], Y.H. Sun[1], W.H. Yu[2], X.Z. Yin[1], J. Weng[1] and B. Feng [1]*

[1] Key Laboratory of Advanced Technology for Materials (Ministry of Education), School of Materials Science and Engineering, Southwest Jiaotong University. Chengdu 610031, China.
[2] College of Chemistry and Materials Science, Sichuan Normal University, Chengdu 610066, China.

## Abstract

Pro-inflammatory phenotype (M1) macrophages initiate angiogenesis, while their prolonged activation can induce chronic inflammation. Anti-inflammatory phenotype (M2) macrophages promote vessel maturation and tissue regeneration. Biomaterials which can promote M2 polarisation after appropriate inflammation should enhance angiogenesis and wound healing. Herein, Interleukin-4 (IL-4), an anti-inflammatory cytokine, was adsorbed onto a titanium surface. Then, a genipin cross-linked gelatine hydrogel was coated onto the surface to delay IL-4 release. The cross-linking degree of the hydrogel was modulated by the different amount of genipin to control release of IL-4. When 0.7 wt% (weight %) genipin was used as a cross-linker, the sample (GG07-I) released less IL-4 within the first several days, followed by a sustained release time to 14 d. Meanwhile, the release rate of IL-4 in GG07-I reached a peak between 3 d and 7 d. In culture with macrophages *in vitro*, GG07-I and GG07 exhibited good cytocompatibility. The phenotypical switch of macrophages stimulated by the samples was determined by FACS, ELISA and PCR. Macrophages cultured with GG07-I, GG07 and PT were firstly activated to the M1 phenotype by interferon-gamma (IFN-γ). Then, due to the release of IL-4 in 5 to 7 d, GG07-I enhanced CD206, increased the secretion and gene expression of M2 marker, such as interleukin-10 (IL-10), arginase-1 (ARG-1) and platelet derived growth factor-BB (PDGF-BB). GG07-I prompted the switch from M1 to M2 phenotype. Those appropriate secretion of cytokines would benefit both vascularisation and osseointegration. Thus, the biomaterial directing inflammatory reaction has good prospects for clinical treatments.

**Keywords:** Genipin cross-linked gelatine, interleukin-4, controlled release, macrophage phenotype polarisation, inflammatory reaction.

***Address for correspondence**: Bo Feng, PhD, Key Laboratory of Advanced Technology for Materials (Ministry of Education), School of Materials Science and Engineering, University of the Southwest Jiaotong University, Jinniu District, Chengdu, China.
Telephone: +86-28-87634023 Email: fengbo@swjtu.edu.cn



## Introduction

Ideal titanium materials for applications such as prosthetic joints should promote blood vessel ingrowth from the surrounding host tissue and connect to the host vasculature (Auger *et al*., 2013; Grayson *et al*., 2010; Laschke MW *et al*., 2012; Novosel *et al*., 2011). Macrophages play an important role in angiogenesis and wound healing (Babensee *et al*., 1998; Brancato and Albina, 2011; Koh and DiPietro, 2011). Once at the wound site, macrophages polarise into M1 macrophages to defend against bacterial infection, contribute to phagocytosis of dead cells, and recruit Th1 cells to the infection site (Daley *et al*., 2010; Epelman *et al*., 2014; Forbes and Rosenthal, 2014; Takemura and Werb, 1984; Yin and Ferguson, 2009). M1 macrophages incite further inflammation by secreting cytokines, such as interleukin-1β (IL-1β), interleukin-6 (IL-6), tumour necrosis factor alpha (TNF-α) and vascular endothelial growth factor (VEGF), to stimulate blood vessel growth (Kanczler and Oreffo, 2008; Martinez and Gordon, 2014). Following the acute inflammatory phase, M2 macrophages emerge at the wound site and act as anti-inflammatory factors by secreting interleukin-10 (IL-10), arginase-1 (ARG-1) and transforming growth factor-beta1 (TGF-β1) to promote extracellular matrix (ECM) synthesis and cell proliferation (Fujisaka *et al*., 2009; Martinez *et al*., 2006; Murray *et al*., 2014). M2 macrophages also secrete platelet-derived

growth factor-BB (PDGF-BB) to stabilise blood vessel growth (Conway *et al.*, 2001). However, unrestrained pro-inflammatory M1 activation releases large amounts of pro-inflammatory cytokines (Tarnuzzer and Schultz, 1996), proteases (Hotamisligil, 2006), and reactive oxygen species (ROS) (Yeoh-Ellerton and Stacey, 2003), which impair the formation of connective tissue and the secretion of essential growth factors (Lauer *et al.*, 2000; Yager *et al.*, 1997). For angiogenesis, administration of VEGF without subsequent PDGF-BB can lead to unstable and leaky vessels (Hellberg *et al.*, 2010; Yancopoulos *et al.*, 2000). In bone healing, inflammation, angiogenesis and new bone regeneration are intimately linked, and the appropriate sequence of the inflammatory stage followed by the anti-inflammatory stage is critical for normal bone healing (Mountziaris and Mikos, 2008).

Sequential release of cytokines is recognised to be important for autorepair of tissues. Some reports currently available focus on regulation of cytokine levels as a strategy to control inflammation or to promote faster healing. Decellularised bone scaffolds, bound with interleukin-4 (IL-4) by biotin-streptavidin interaction, are used to promote vascular genesis and control macrophage polarisation (Spiller *et al.*, 2015). Carvalho *et al.* encapsulate IL-10 into a dextrin self-assembled nanogel, and the nanogel enables the release of biologically significant amounts of IL-10 (Carvalho *et al.*, 2010). Silk protein is used to form a biopolymer film that releases either interferon gamma (IFN-γ) or IL-4 to control macrophage polarisation (Reeves *et al.*, 2015). The development of controlled release strategies shows that it is feasible to modulate M1-M2 polarisation. In the current study, a strategy was designed to ensure the dominance of M1 macrophages at early stages (1-3 d) after an injury and the dominance of M2 macrophages at later stages (5-7 d).

Gelatin hydrogel is an ideal biomaterial for tissue engineering because it is biocompatible, non-toxic, non-immunogenic, cheap and biodegradable (Bigi *et al.*, 2002; Young *et al.*, 2005). Gelatine hydrogel is used in the form of disks for delivery of several growth factors, including basic fibroblast growth factor (bFGF) and TGF-β1 (Santoro *et al.*, 2014). Cross-linking treatments can improve its mechanical properties and adjust its solubility. Genipin is a potent and non-toxic cross-linker of proteins with anti-inflammatory properties (Koo *et al.*, 2004; Koo *et al.*, 2006; Mi *et al.*, 2000). Genipin is known to cross-link gelatine by the epsilon amino group present in lysine and hydroxylysine residues (Nickerson *et al.*, 2006), and cross-linked hydrogels are employed in nerve-guiding conduits, wound dressings, and cartilage scaffolds (Chen *et al.*, 2005; Lien *et al.*, 2008).

In the current study, cross-linked coatings on acid-alkali-treated titanium that released the M2-promoting cytokine IL-4 at the later stage (5-7 d) following injury, were designed. The biodegradability of the prepared coatings and the release behaviour of IL-4 were evaluated in this research. A simulated inflammatory microenvironment was generated by the M1-promoting cytokine IFN-γ. Then, the ability of the designed biomaterials to polarise M1 macrophages to M2 phenotypes was demonstrated *in vitro* and was confirmed by gene expression, surface marker expression and protein secretion analyses. As shown in Fig. 1, the sequential immunoreactions of the macrophages on the designed biomaterials *in vitro* were further assessed for a comprehensive understanding of the induced osteo-immunomodulation.

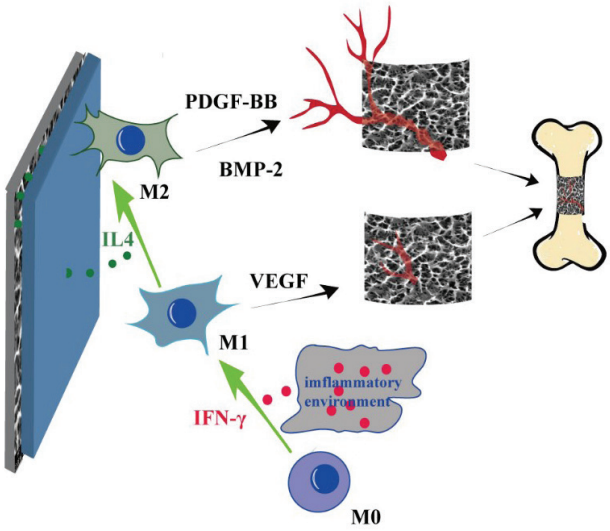


**Fig. 1. Schematic illustration of macrophage regulation for improving osteogenesis and angiogenesis on GG07-I surfaces.**

## Materials and Methods

### Surface pretreatment

Commercial pure titanium disks, denoted as pure titanium (PT), 10 mm in diameter (Northwest Institute for Non-Ferrous Metal Research, Ningxia, China) were polished and pre-treated with mixed acid (6.0 M $HNO_3$ and 1.0 M HF). Acid-etching was carried out by soaking the PT in a 2 M HCl solution for 2 h at 60 °C. Then, alkali treatment was carried out in a 5 M NaOH solution at 60 °C for 24 h followed by washing and drying. The resulting disks are denoted as AAT.

### Gelatine hydrogel preparation and IL-4 immobilisation

A 5 % genipin solution was prepared by dissolving 0.5 g of genipin (Challenge Bioproducts, Taichung, Taiwan) in 9.5 mL of 60 % ethanol. Type A gelatine (Sigma, St. Louis, MO, USA), with an average molecular weight of between 50,000 and 100,000 Da, was extracted from porcine skin. The gelatine solution was obtained by dissolving 10 g of gelatine in 90 mL of distilled water at 60 °C and then mixing the gelatine solution with the genipin solution to obtain gelatine-

genipin mixtures with 0.3, 0.7 and 1.2 weight % (wt%) genipin. Recombinant murine IL-4 (Peprotech, NJ, USA) was loaded onto the titanium surface using the following method. First, 20 μL of the IL-4 solution (10 μg/mL) was dripped onto AAT. After drying, the AAT samples with IL-4 were coated with 120 μL of the aforementioned gelatine-genipin mixtures. The mixtures were cross-linked for 24 h to form hydrogels at 37 °C, and then, the reaction was terminated by the addition of glycine (25 mg/mL). The degree of cross-linking of the hydrogels was measured using ninhydrin assays (Lai, 2013; Yao *et al.*, 2004) and expressed as a percentage of free amino groups lost during cross-linking. The samples were repeatedly washed with double distilled water and then lyophilised. The resulting samples with different hydrogel coatings (genipin at 0.3, 0.7, or 1.2 wt%) were denoted as GG03-I, GG07-I and GG12-I, and the samples without IL-4 were denoted as GG03, GG07 and GG12.

**Surface characterisation**

The surface morphology was investigated using thermal field emission scanning electron microscopy (FESEM, JSM-7001F, JEOL, Japan). Water contact angles were measured with a Krüss GmbH DSA 100 Mk2 goniometer (Hamburg, Germany) with image processing of a sessile 5 μL drop of ultrapure water. Surface chemical compositions were measured by Fourier transform infrared spectroscopy (Bruker, Nicolet 5700, Beijing, China).

*In vitro* **degradation and release**

Phosphate-buffered saline (PBS) and collagenase-containing PBS were used for degradation and release tests of the prepared samples, respectively. The collagenase solution was prepared from lyophilised collagenases isolated from *Clostridium histolyticum* (Sigma, USA) and diluted in PBS to a concentration of 10 units/mL. The samples were incubated in a 24-well plate containing 1 mL of the above solution at 37 °C and agitated at 70 rpm. The extent of degradation ($D$) was calculated as follows:

$$D = \left(1 - \frac{m_t}{m_0}\right) \times 100\%$$

where $m_t$ is the mass of the sample at a particular time point, and $m_0$ is the initial mass. All samples were lyophilised before being weighed at each time point. After 7 d, the samples were taken out and dried for SEM observation. Mouse IL-4 enzyme-linked immunosorbent assay (ELISA) kits (Neobiosience, Shenzhen, China) were used to measure the concentration of IL-4 released from GG03-I, GG07-I and GG12-I in both release media, according to the manufacturer's protocol.

**Cell culture and viability**

The murine-derived macrophage cell line (RAW 246.7) was cultured in Dulbecco's modified Eagle's Medium (DMEM, HyClone, Logan, Utah, USA) supplemented with 10 % heat-inactivated foetal bovine serum (Biological Industries, Kibbutz Beit Haemek, Israel). Macrophages were seeded onto the sample surfaces at a density of $5 \times 10^4$ cells/cm$^2$ in 1 mL of the abovementioned medium containing 30 ng of IFN-γ to induce M1 polarisation. Macrophages cultured on PT were used as a control. On the third day, the polarisation medium was changed to medium without IFN-γ. Cell viability was determined using the alamar blue (Invitrogen, Thermo Fisher Scientific) assay at the designated time points (1, 3, 5 and 7 d for macrophages). Optical density (OD) was measured at 570 nm on a microplate reader (Biotek, CA, USA), with 600 nm as the reference wavelength.

**Cell adhesion and morphology**

After 1, 3, 5 and 7 d of incubation, samples with macrophages were washed and then fixed with 2.5 % glutaraldehyde at 4 °C overnight. For cytoplasmic and nuclear staining, samples were stained with 1 μg/mL fluorescein isothiocyanate (FITC)-phalloidin for 10 min and 1 μg/mL 4',6-diamidino-2-phenylindole (DAPI) for 5 min after being washed with PBS. Fluorescence images were captured with a Leica DMRX fluorescence microscope. The number of adherent cells was determined from 5 images of randomly selected areas in the samples. The surface morphology of cells was investigated using FESEM.

**Flow cytometric analysis**

After 3 and 7 d of incubation, macrophages were digested with trypsin (without ethylenediaminetetraacetic acid). Analysis of each sample was performed in triplicate. After centrifugation, macrophages were dual-stained with PerCP-Cy5.5-conjugated chemokine receptor CCR7 (Molecular Probes™, A18396, dilution 1:50) and FITC-conjugated mannose receptor CD206 (Invitrogen, MA5-16870, dilution 1:100) antibodies. Labelled cells were detected by flow cytometry using a FACSCalibur instrument and CellQuest software (Beckman Coulter, IN, USA). The data were analysed with FlowJo software (FlowJo LLC, Ashland, Oregon, USA).

**ELISA assay**

At 1, 3, 5 and 7 d, the cytokines (TNF-α, IL-1β, IL-6, IL-10, TGF-β1, and VEGF) secreted by macrophages were detected using ELISA kits (Neobiosience) according to the manufacturer's instructions.

**RT-PCR assay**

To analyse gene expression, cells were lysed with RNAiso Plus reagent (TaKaRa, Dalian, China) at 3 and 7 d. To generate cDNA, PrimeScript™ RT Master Mix (TaKaRa) was used for reverse transcription according to the manufacturer's instructions. Real-time polymerase chain reaction (RT-PCR) primers (Table 1) were designed based on cDNA sequences from the NCBI Sequence Database and synthesised by TsingKe Biological Technology. RT-qPCR was

performed with SYBR® Premix Ex Taq™ II (TaKaRa) using the following protocol: 95 °C for 30 s, 40 cycles of PCR (95 °C for 5 s, 60 °C for 30 s) and a melt curve (95 °C for 10 s, 65 °C for 5 s and 95 °C for 5 s). The mRNA expression of targets was assayed on a CFX96 Real-Time Detection System (Bio-Rad, CA, USA) using glyceraldehyde-3-phosphate dehydrogenase (GAPDH) as the internal control. Analysis of each sample was performed in triplicate. For calculation of fold change, the $2^{-\Delta\Delta Ct}$ method was applied, compared with the mRNA expression in macrophages cultured on PT.

**Table 1.** The primer sequences used in RT-qPCR.

| Name | 5′-Sequence-3′ |
|---|---|
| TNF-$\alpha$ | forward CTGTAGCCCACGTCGTAGCAA |
| | reverse TGTCTTTGAGATCCATGCCGTT |
| IL-10 | forward GAGAAGCATGGCCCAGAAATC |
| | reverse GAGAAATCGATGACAGCGCC |
| ARG-1 | forward ATCAACACTCCCCTGACAACC |
| | reverse TCGCAAGCCAATGTACACGAT |
| BMP-2 | forward GCCCATTTAGAGGAGAACCCA |
| | reverse GCTTGACGCTTTTCTCGTT |
| PDGF-BB | forward TCTCTGCTGCTACCTGCGTCT |
| | reverse CAGCCCCATCTTCATCTACGG |
| VEGF | forward GTCCCATGAAGTGATCAAGTTC |
| | reverse TCTGCATGGTGATGTTGCTCTCTG |
| GAPDH | forward AGAACATCATCCCTGCATCCAC |
| | reverse TCAGATCCACGACGGACACA |

### Statistical analysis

Statistical analyses were performed using SPSS Statistics 19.0 (IBM, Armonk, NY, USA). All the quantitative data was presented as mean and standard deviation. The statistical significances were evaluated using non-parametric Kruskal-Wallis one-way analysis of variance by ranks, and with Mann-Whitney *post hoc* test combined with Bonferroni correction. Significance was indicated at adjusted $p$-value < 0.05.

## Results

### Surface characterisation

Among the gelatine coatings on titanium surfaces (such as GG07 in Fig. 2**a**), GG07 exhibited the same hydrophilicity as PT and slightly lower hydrophilicity than gelatine, due to crosslinking. The surface water contact angles of GG03 and GG12 were 72.21° ± 3.12 and 73.75° ± 2.67, respectively. The FTIR spectra of GG03 and GG12 were almost the same as that of GG07 (Fig. 2**b**). Two reactions proceeded in the formation of crosslinks with the primary amine groups of gelatine. One reaction was a nucleophilic attack on genipin by a primary amine group of gelatine, which led to the formation of a heterocyclic. The other reaction was nucleophilic substitution of the ester group on genipin to form an amide linkage with gelatine. The peaks at 1620 $cm^{-1}$ and 1556 $cm^{-1}$ of GG07, attributed to the amide I band and the amide II band vibration, respectively, indicated that the nucleophilic substitution occurred. The peak at 1400 $cm^{-1}$, attributed to a ring stretching mode of genipin, indicated that genipin was successfully crosslinked in GG07. After genipin crosslinking, C-N

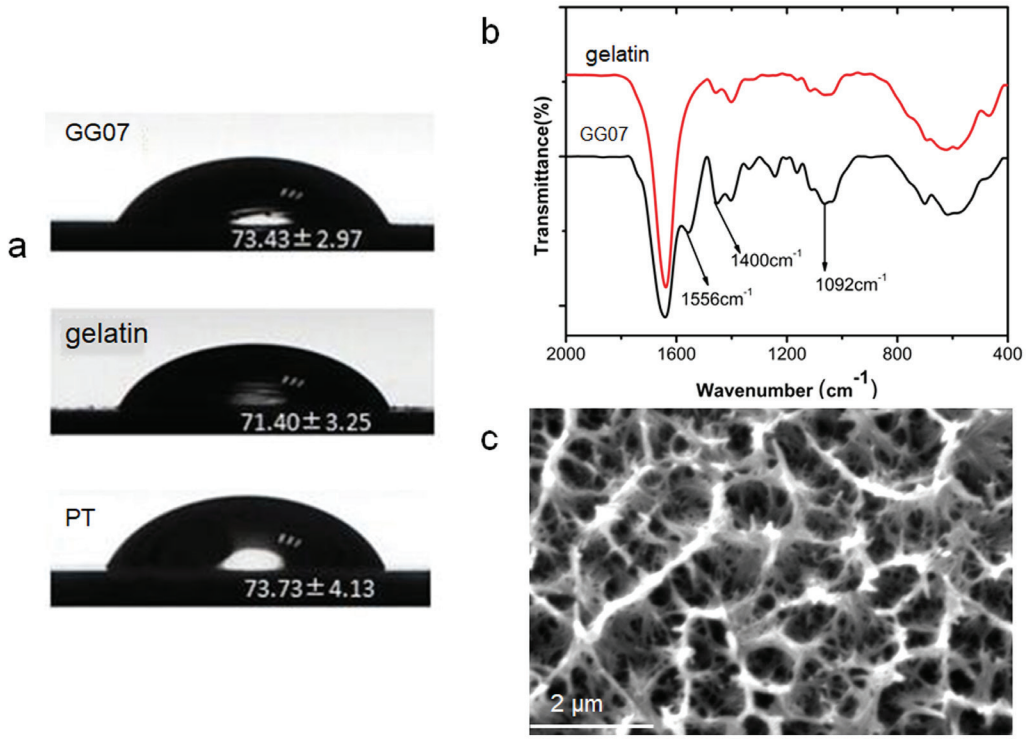


**Fig. 2. Properties of PT, GG07, gelatine and AAT**. (**a**) Surface water contact angles of PT, GG07 and gelatine. $n$ = 3. (**b**) The FTIR spectra of GG07 and gelatine. (**c**) Surface morphology of AAT.

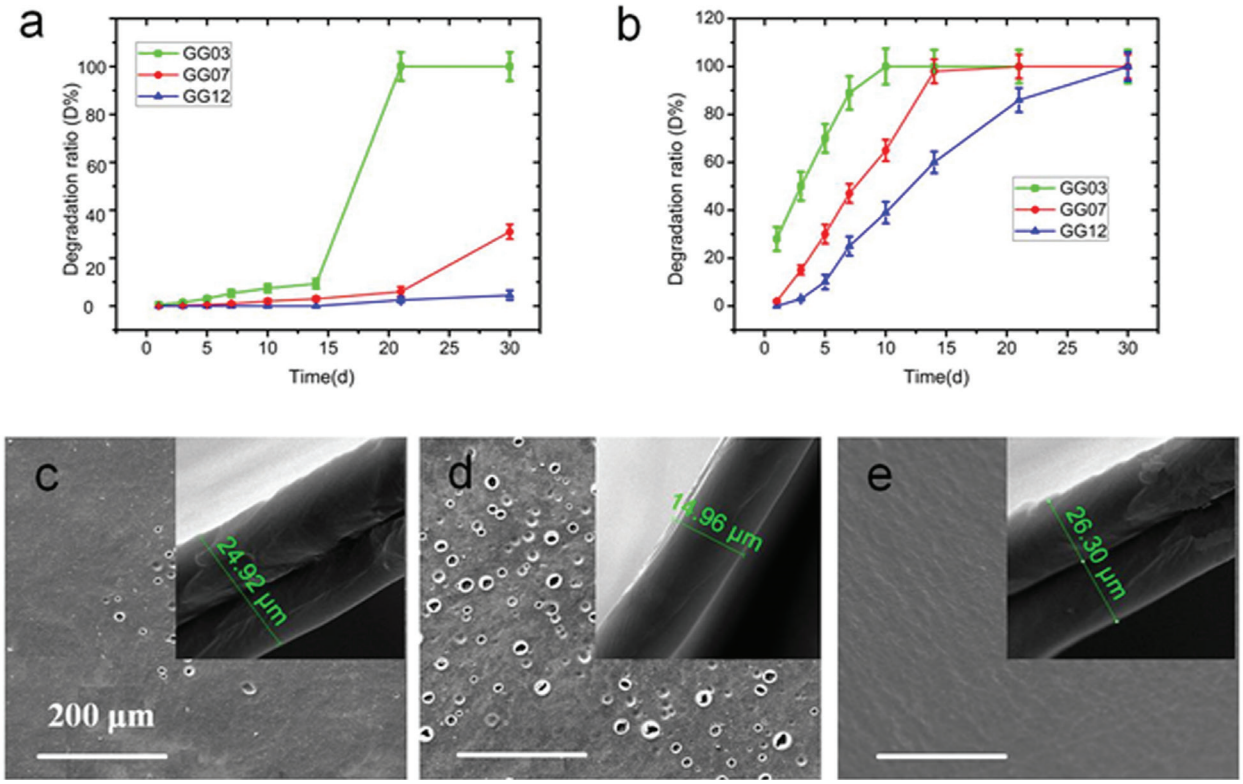


**Fig. 3. Degradation of GG07**. (**a**) Degradation profile in PBS. $n = 4$. (**b**) Proteolytic degradation profile in PBS containing collagenase. $n = 4$. (**c**) Surface morphologies of GG07 after 7 d of degradation in PBS. (**d**) Surface morphology of GG07 after 7 d of degradation in PBS containing collagenase. (**e**) Surface morphology of GG07 before degradation. A cross-section of the sample is shown in the insert.

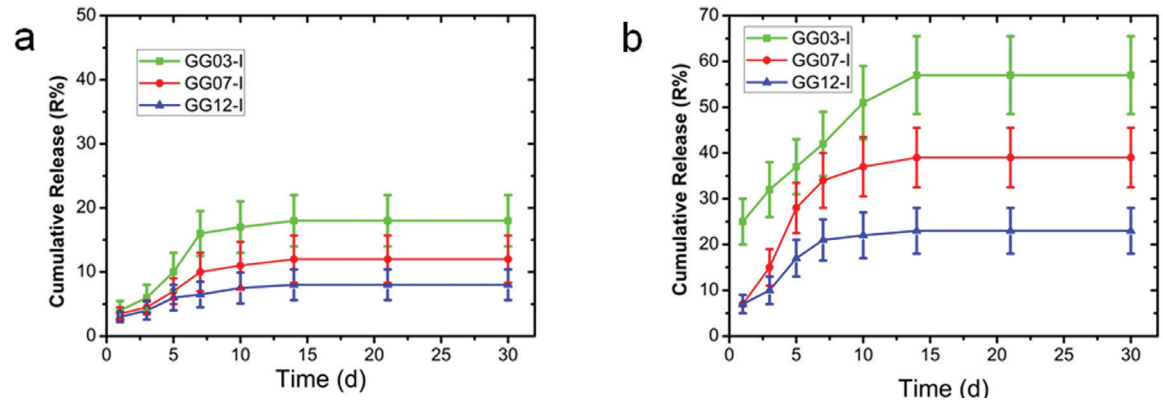


**Fig. 4. Release of IL-4**. Cumulative release of IL-4 (**a**) in PBS and (**b**) in PBS containing collagenase. $n = 3$.

bonds (1092 $cm^{-1}$) formed in GG07 by nucleophilic attack. The rich macro-nanostructures (Fig. 2**c**) and good hydrophilicity, making AAT an excellent reservoir for delivering IL-4.

### *In vitro* degradation

The cross-linking indexes of the hydrogels coated on GG03, GG07 and GG12 were 65 ± 4, 80 ± 3 and 86 ± 3, respectively. The degradation ratio (D%) in both degradation solutions was obtained over 30 d (Fig. 3). Due to the low cross-linking index, no significant mass loss was detected while hydrogels were immersed in PBS for 14 d, except for GG03. Macrophages are well known for participating in extracellular biodegradation of extracellular matrices by releasing a spectrum of enzymes, such as collagenase. Here, PBS buffer containing collagenase was used as a degradation solution to simulate the microenvironment *in vitro*. Samples immersed in the collagenase solution were observed to lose mass at two stages, referred to as the steady and tailing periods. In the steady state, samples began to degrade with increasing collagenase infiltration. Moreover, the degradation rate was the fastest in this period and was associated with the degree of cross-linking. In the tailing period, the degradation rate decreased. The total proteolytic degradation time of GG03, GG07 and GG12 was 10 d, 14 d and 28 d, respectively. Notably,

the proteolytic degradation ratios of GG07 and GG03 were higher than that of GG12 between 3 and 7 d. Meanwhile, only approximately 15 % weight loss of GG07 due to proteolytic degradation was detected in the first 3 d.

After 7 d of degradation, the proteolytic GG07 sample lost its integrity and many 2-20 μm holes could be seen on the surface, in contrast with the hydrolytic samples. The thickness of the hydrogel layer of GG07 for the proteolytic sample was approximately 15 μm, compared with the hydrolytic sample with a thickness of approximately 25 μm (Fig. 3). The number of holes and the thickness change of the hydrogel were in good accordance with the proteolytic degradation profiles.

*In vitro* **release**

GG07-I allowed for large amounts of IL-4 release from 3 to 7 d and smaller amounts of release within 3 d. The IL-4 release was increased with the addition of collagenase to the buffer and the decrease of cross-linking extent. In PBS without collagenase (Fig. 4**a**), the slight IL-4 release corresponded to the insignificant degradation profile (Fig. 3**a**). With an increased degree of cross-linking (65 ± 4 %, 80 ± 3 %, and 86 ± 3 %), the hydrogel exhibited a more compact gel network. Therefore, the release of IL-4 decreased in the simulated microenvironment *in vitro* (Fig. 4**b**). With increasing collagenase infiltration, the hydrogel began to crack. A burst release (25 %) from GG03-I was observed at 24 h, compared with the initial release of 7 % from GG07-I and GG12-I. The release rate of GG07-I was obviously faster than that of GG12-I between 3 and 7 d. Within 7 d, approximately 30 % of the IL-4 was released from GG07-I, while the release from GG12-I was approximately 20 %. The IL-4 release from GG03-I occurred in a burst release, while GG07-I exhibited a minimal burst release followed by a more sustained release until 14 d. GG12-I exhibited a decrease in the total release amount. Thus, GG07-I appeared suitable for an IL-4 delivery device, where the presence of IL-4 would be desired 3 d post-inflammation, with a subsequent decrease and disappearance of IL-4 to avoid fibrous encapsulation of biomaterials.

**Inflammatory response**

*Macrophage viability, adhesion and morphology*

The cell viability profile showed that there were significant differences among the three groups of samples after being cultured for 1, 3 and 5 d. Macrophage viability increased in the first 5 d and then decreased at 7 d (Fig. 5**a**). Overall, macrophages on GG07-I and GG07 showed higher viability than those on PT, which indicated good cytocompatibility of the cross-linked hydrogel.

Macrophage adhesion, quantity and distribution on the sample surfaces were observed using FM (Fig. 5**b** and Fig. 6) and SEM (Fig. 7). The initial number of adherent macrophages on GG07-I and GG07 surfaces were higher than those on PT, as shown in (Fig. 5**b**). The adherent cell density reached a peak at 5 d for all samples and then decreased. Fig. 6 and Fig. 7 show the morphologies of macrophages attached to the material surfaces at various culture times. F-actin in macrophages was stained green with FITC-phalloidin. Once activated, migratory cells contained abundant F-actin, especially in lamellipodia and filopodia. As shown in Fig. 6, most cells exhibited a discoid shape. At 1 d, the cells on all samples began to exhibit good cell-cell adhesion. The cell-cell adhesion increased significantly with fusion areas at 3 d. Meanwhile, cell-surface adhesion increased significantly, with a larger spread area at 3 d and 5 d, and more abundant F-actin and pseudopodia appeared on cells adhered to GG07-I surfaces. Then, the size of adherent cells decreased until 7 d, compared with the previous few days.

As shown in the SEM images (Fig. 7), macrophages presented a discoid shape on the material surfaces at 1 d and 3 d. At 5 d, macrophages on GG07-I became spindle-shaped with more pseudopodia and more abundant F-actin. Within 5 d, approximately 27 % of the IL-4 was released from GG07-I (Fig. 4**b**), suggesting that the release of IL-4 may be the reason for the morphology change. At 7 d, the macrophages

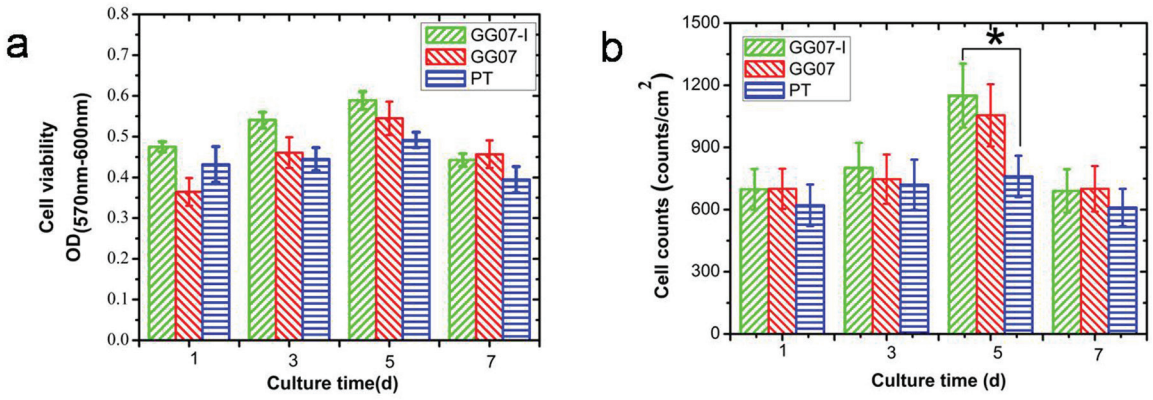


**Fig. 5. Macrophage viability and counts**. (**a**) Macrophage viability on material surfaces after culture for 1, 3, 5 and 7 d. $n = 3$. (**b**) The number of macrophages attached on GG07-I, GG07 and PT at 1, 3, 5 and 7 d. $n = 5$, * $p < 0.05$.

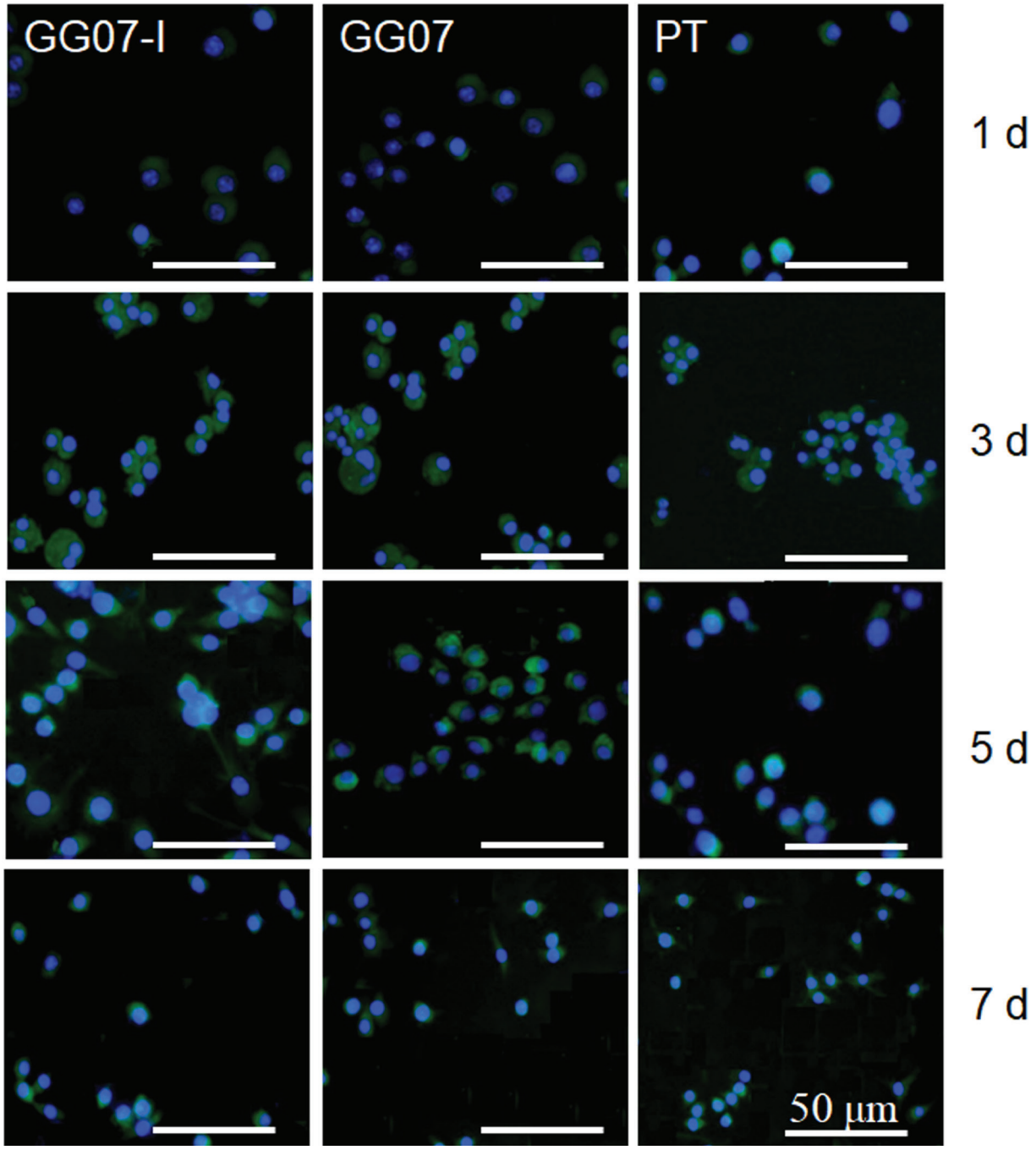


**Fig. 6. Fluorescence images of macrophages**. Fluorescence images of macrophages on GG07-I, GG07 and PT after 1, 3, 5 and 7 d. Cells were stained with DAPI (blue) and FITC-phalloidin (green).

contracted and tended to round in shape with obviously decreased pseudopods. In a previous study, the surface topography of PT significantly changes after culture with macrophages. The micron pits on the PT surface disappear as cultivation time is prolonged, with some convex structures exposed (Sun *et al.*, 2017) because the active macrophages secrete proteolytic enzymes and reactive oxygen species onto the biomaterial surface. Collagenases and gelatinases are detected in macrophages adhered to collagen disks post ex-plantation (Luttikhuizen *et al.*, 2006; MacLauchlan *et al.*, 2009). It is suggested that the combined action of both gelatinases and collagenases promotes degradation of coatings on implants. Then, macrophages gain access to the cytokines loaded into the sample. In the current study, we investigated hydrogel changes after culture with macrophages. After being cultured on GG07-I for 3 d, macrophages were removed from the attached sample by trypsinisation, and then GG07-I was dried for SEM imaging (Fig. 7 insert). Many small pits appeared in areas where cells had been attached and in the surrounding area, suggesting degradation of the hydrogels by macrophages.

*Macrophage phenotypes*

CCR7 and CD206 are surface markers of different macrophage phenotypes. M1 macrophages up-

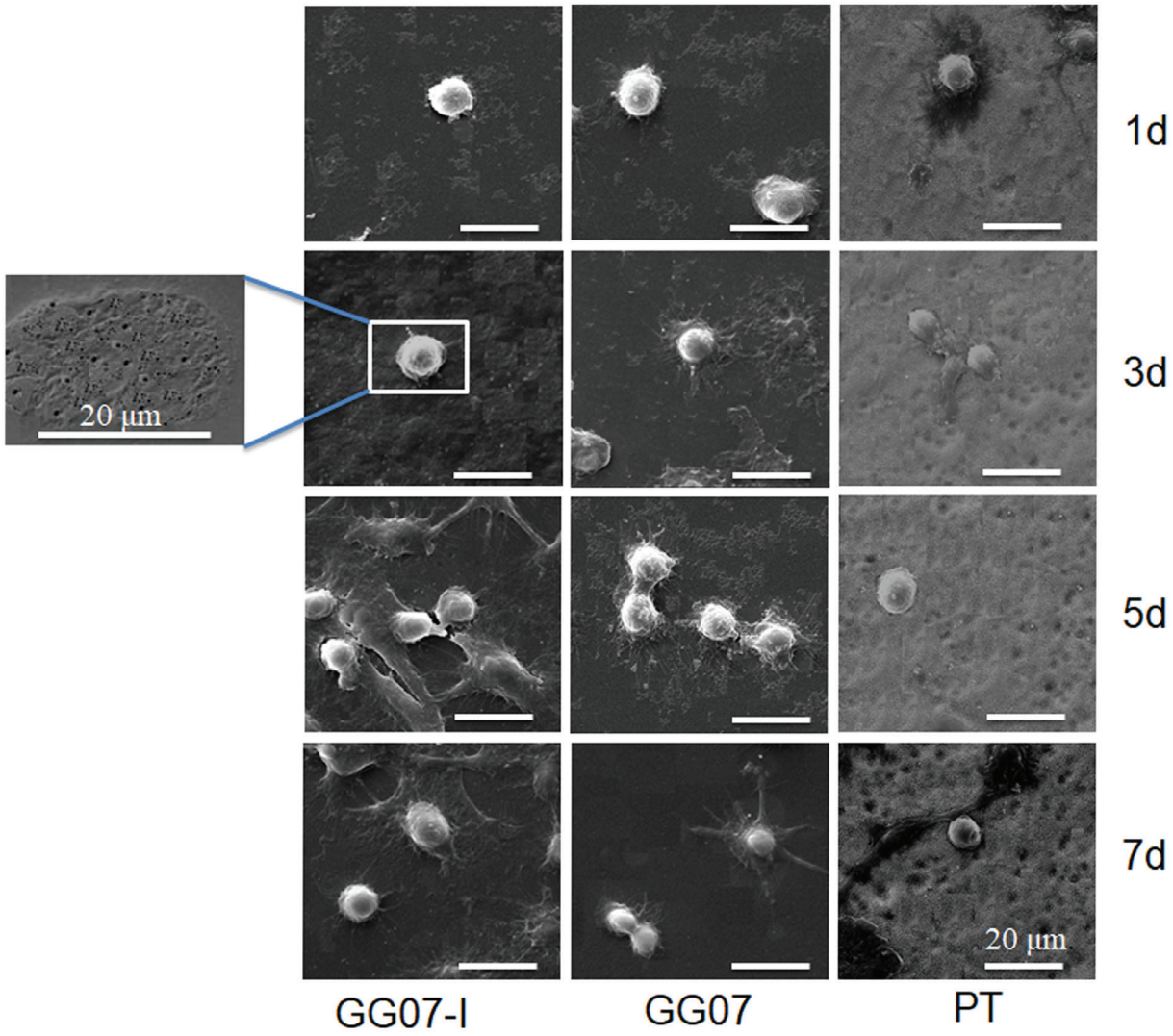


**Fig. 7. Scanning electron microscopy**. SEM images of macrophages adherent to the GG07-I, GG07 and PT surfaces after 1, 3, 5 and 7 d. SEM image of cell cultured on GG07-I removed by trypsin at 3 d is shown in the insert.

regulate CCR7, while M2 macrophages up-regulate CD206 (Spiller *et al*., 2014). Flow cytometric analysis was used to determine CCR7 and CD206 expression in macrophages cultured on GG07-I, GG07 and PT for 3 and 7 d. CCR7 and CD206 expression at 3 d was not significantly different among the material groups (Fig. 8). Macrophages cultured on GG07 and PT exhibited almost the same level of CCR7 and CD206 expression at 7 d. Macrophages on GG07-I exhibited increased CD206 expression and decreased CCR7 expression. As expected, the addition of IFN-γ induced strong CCR7 up-regulation at 3 d, in contrast with the expression at 7 d (Fig. 8). The up-regulation of CD206 on GG07-I coincided with the cumulative release of IL-4 in the sample at 7 d (Fig. 4**b**). The same expression levels between GG07 and PT macrophages showed that the cross-linked hydrogel had no additional effect on macrophage polarisation, compared with the titanium substrate. All these data indicated that IL-4-loaded samples induced a phenotype switch from M1 to M2 at 7 d.

The amounts of secreted proteins associated with M1 and M2 phenotypes were measured by ELISA to support the flow cytometric results (Fig. 9). For the pro-inflammatory cytokines IL-1β, IL-6 and TNF-α, the expression levels declined with culture time. Additionally, GG07-I macrophages exhibited lower pro-inflammatory cytokine expression levels than GG and PT macrophages. The inflammatory cytokines IL-1β, IL-6 and TNF-α, secreted by M1 macrophages, have been shown to prime endothelial cells for sprouting by promoting the tip cell phenotype and to stimulate endothelial cells to recruit supporting pericytes. For the anti-inflammatory cytokines IL-10 and TGF-β1, the expression in macrophages on GG07-I increased with culture time, especially from 5 to 7 d. While the expression in macrophages on GG07 and PT was not significantly different, Fig. 4**b** shows that IL-4 was released in a large amount at 5 to 7 d, and as a result, the macrophages on GG07-I were polarised to the M2 phenotype and secreted more anti-inflammatory cytokines.

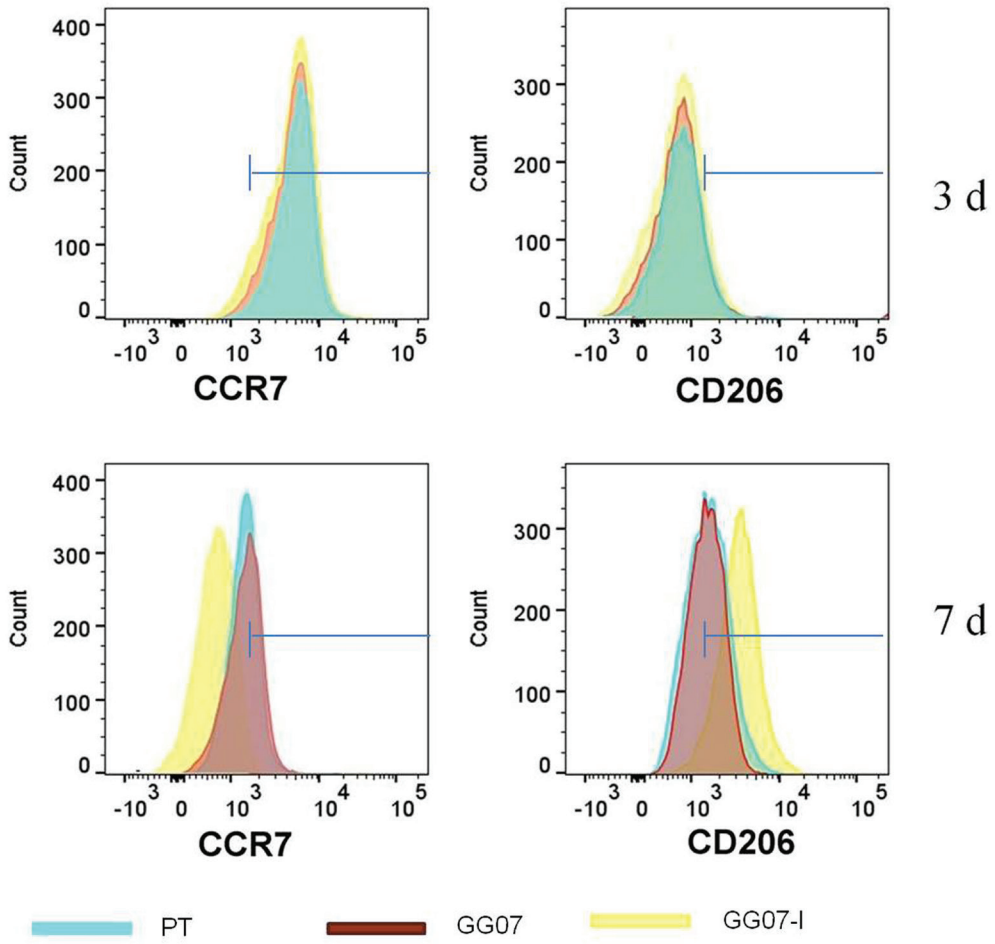


**Fig. 8. Flow cytometry**. Flow cytometric analysis of the macrophage phenotype markers CCR7 showed a positive expression on PT (93.7 ± 4.2 %), GG07 (91.0 ± 3.0 %), GG07-I (89.3 ± 3.1 %) at 3 d and a negative expression on PT (46.0 ± 1.9 %), GG07 (42.9 ± 1.9 %), GG07-I (9.8 ± 0.7 %) at 7 d. FACS analysis of the macrophage phenotype markers CD206 showed a negative expression on PT (9.5 ± 0.7 %), GG07 (9.9 ± 0.9 %), GG07-I (12.0 ± 1.2 %) at 3 d and a positive expression on PT (52.9 ± 2.0 %), GG07 (54.4 ± 2.1 %), GG07-I (89.9 ± 3.1 %) at 7 d.

M1 macrophages secrete cytokines, including VEGF, involved in the initiation of angiogenesis (Spiller *et al.*, 2014). The secretion of VEGF was confirmed at the protein level (Fig. 9**f**). Upon initial inflammatory stimulation by IFN-γ, macrophages quickly secreted inflammatory factors, and VEGF expression peaked at 1 d. Then, the level of secretion declined at 3 d, which might have been related to the secretion of other cytokines. Meanwhile, GG07-I macrophages secreted more VEGF than GG07 and PT macrophages. VEGF, at the initial inflammatory stage, is beneficial for angiogenesis initiation. We presumed that the release of IL-4 stimulated VEGF secretion. At 5 d, without IFN-γ in the culture medium, the activity of the M1 phenotype decreased, resulting in a low level of VEGF for the three samples. At 7 d, besides GG07 and PT, GG07-I caused a significant increase in VEGF, which corresponded to the high secretion level of IL-10 and TGF-β1 at 5-7 d. This phenomenon supported the proposal that IL-4 released by GG07-I began to activate the M2 phenotype.

Additionally, real time-PCR was used to verify the polarisation status (Fig. 10). Gene expression analysis of macrophages cultured on GG07-I (Fig. 10**a-c**) indicated a low level of pro-inflammatory TNF-α and high levels of anti-inflammatory ARG-1 and IL-10 at 7 d. The results were in good accordance with the release profile *in vitro*, which indicated that approximately 30 % of the IL-4 was released from GG07-I within 7 d. BMP-2 is well known as a morphogen that induces osteogenesis (Kanczler *et al.*, 2008). BMP-2 gene expression was higher at 7 d than at 3 d, indicating that the cross-linked hydrogel was beneficial for osteogenesis. The expression of PDGF-BB, which is involved in angiogenesis, was similar to that of VEGF. With regard to the expression of VEGF and PDGF-BB, both samples were almost the same, due to the same stimulation by IFN-γ at 3 d, which then increased at 7 d. GG07-I macrophages showed higher levels of VEGF and PDGF-BB expression at 7 d than GG07 macrophages (Fig. 10**e-f**). For the ability of GG07-I to support angiogenesis, a high level of VEGF

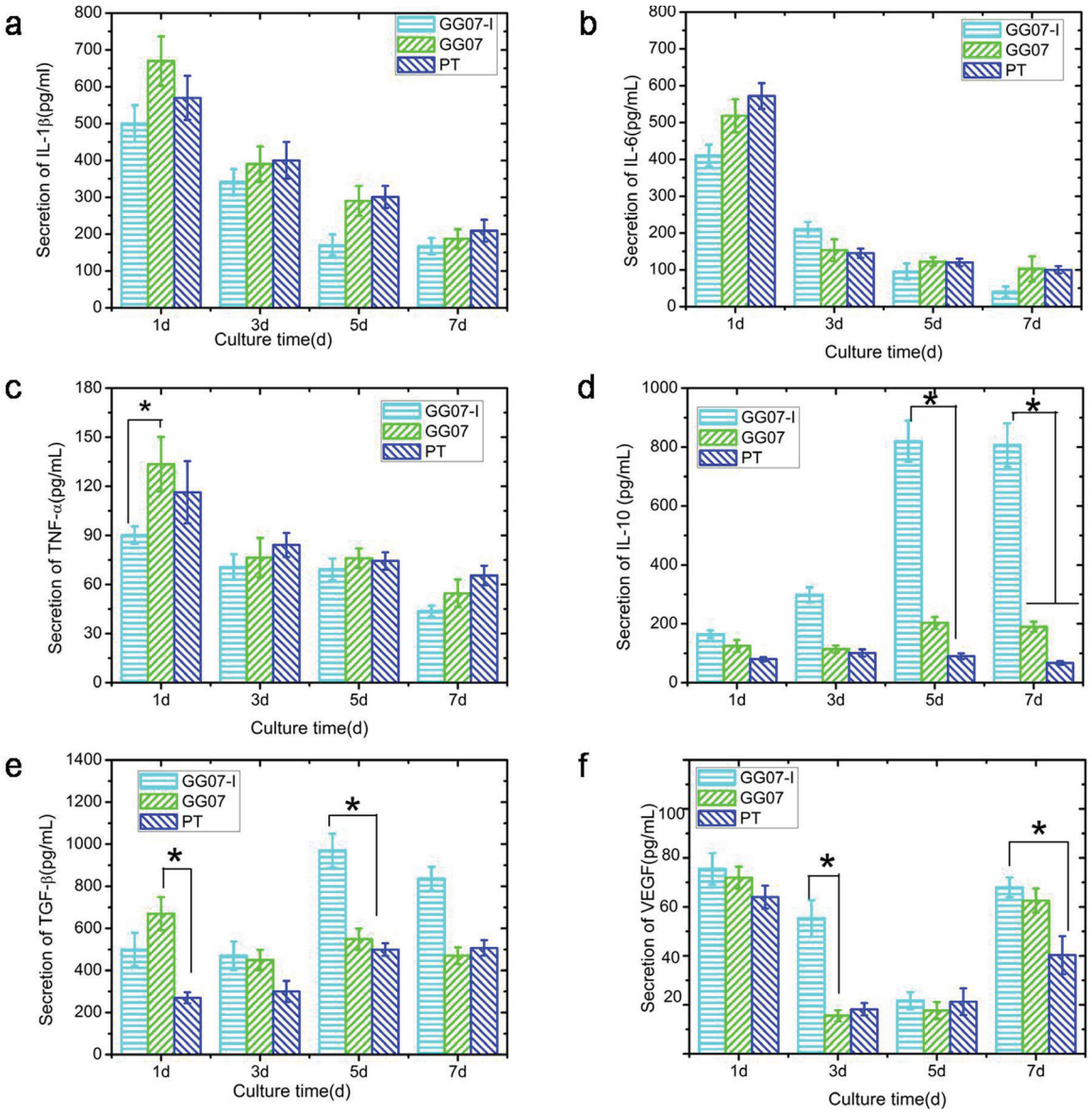


**Fig. 9. Cytokine and growth factor secretion**. Secreted levels of (**a**) IL-1β, (**b**) IL-6, (**c**) TNF-$\alpha$, (**d**) IL-10, (**e**) TGF-β1 and (**f**) VEGF in the supernatants of macrophages cultured on different surfaces for 1, 3, 5 and 7 d. $n = 3$, * $p < 0.05$.

administered with subsequent PDGF-BB could lead to stable vessels.

## Discussion

Using synthetic materials to stimulate tissue self-healing by simulating the body's natural immune reactions is a promising strategy. Tissue regeneration and healing are destined to undergo the inflammatory response and angiogenesis after implantation of biomaterials (Madden *et al.*, 2010; Roh *et al.*, 2010; Spiller *et al.*, 2014). M1 macrophages followed by M2 macrophages, sequentially, achieve greater vascularisation and healing. Localised delivery systems provide the means to modulate immune responses. In this study, the anti-inflammatory cytokine IL-4 was encapsulated in a cross-linked gelatine hydrogel on AAT surfaces. The hydrogel layer achieved a controlled and sustained release of IL-4 to initiate the shift from M1 to M2 macrophages at a later stage (5-7 d).

Preparation of the hydrogel layer was simple, and the cross-linking mechanism of the hydrogel was confirmed by FTIR. Importantly, the hydrogel preserved cytokine stability and could release IL-4 in a controlled manner. The release of IL-4 was dependent upon the extent of hydrogel cross-linking and the microenvironment of the release site. In PBS, the release of IL-4 was due to the swelling of the hydrogels and diffusion of IL-4 itself. The addition of collagenase to the medium increased IL-4 release compared with PBS alone. In the presence of collagenase, the hydrogel cross-linked with a high concentration of genipin exhibited a more compacted dimensional network and released a lower amount

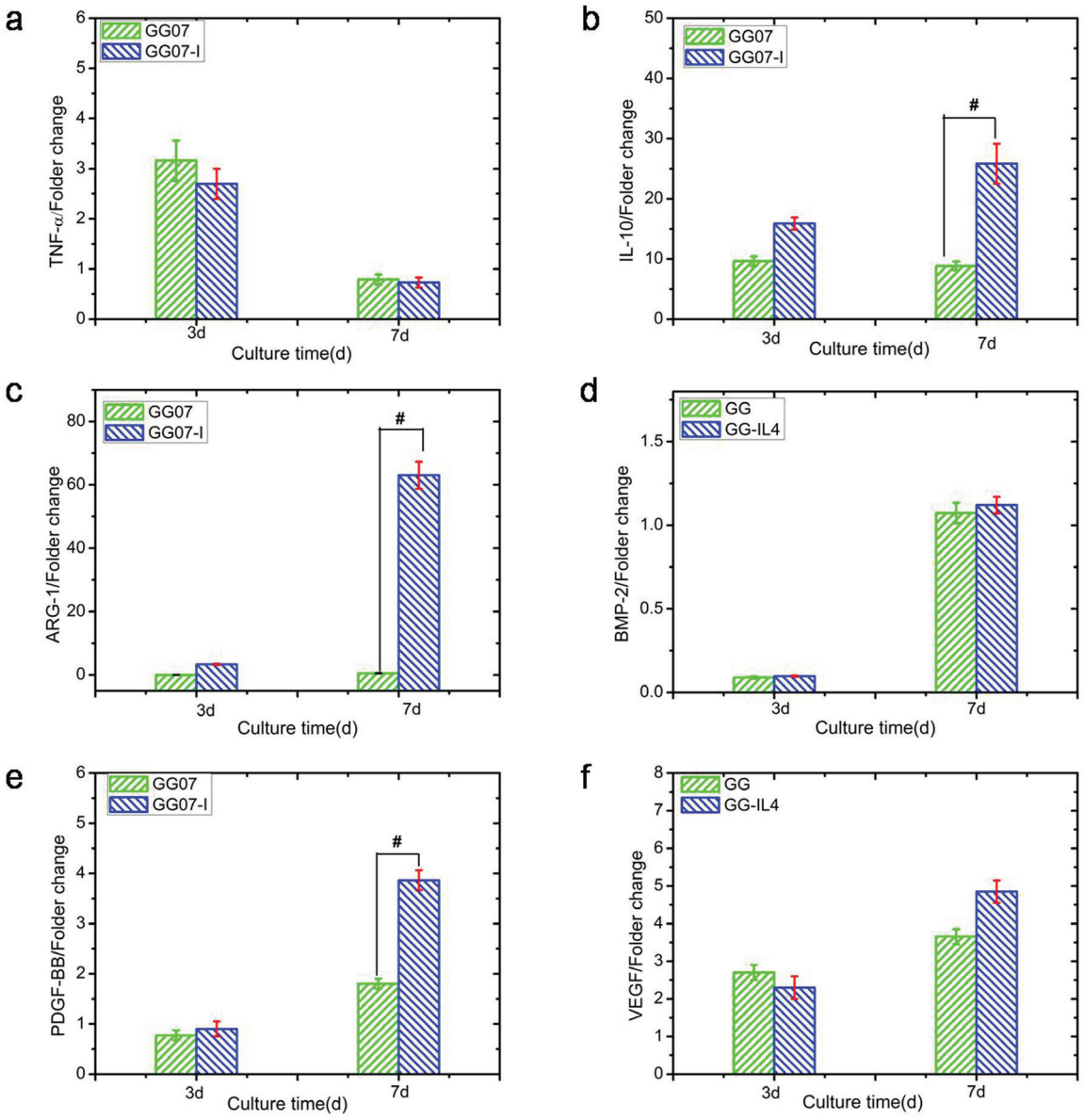


**Fig. 10. Cytokine and growth factor gene expression**. Gene expression of (**a**) TNF-α, (**b**) IL-10, (**c**) ARG-1, (**d**) BMP-2, (**e**) PDGF-BB and (**f**) VEGF analysed by RT-PCR after 3 and 7 d of culture. $n = 3$, # $p < 0.05$.

of IL-4. GG03-I exhibited an approximately 56 % cumulative release and a 25 % initial burst release. GG12-I exhibited only an approximately 23 % cumulative release. The optimal hydrogel, GG07-I, allowed large release amounts at 5-7 d without an initial burst release.

The macrophage cell culture indicated good biocompatibility of the hydrogels compared with PT. The fluorescence analysis showed good expansive cell morphologies on the samples. GG07-I promoted initial attachment and spreading, which is beneficial to induce neovascularisation *in vivo* (Fakhry *et al.*, 2004; LogithKumar *et al.*, 2016). Although hydrophilic surfaces are reported to reduce macrophage adhesion and inflammatory activity (Brodbeck *et al.*, 2001; Brodbeck *et al.*, 2002), in the present work, the hydrophilicity of the hydrogel and PT were nearly the same. Therefore, the initial increase in macrophage adhesion on the hydrogel probably depended on the abundant functional groups in the gelatine matrix, which facilitated protein adsorption and cell adhesion.

Macrophage phenotypes can be defined by gene expression patterns and secreted proteins. Based on the analysis of the surface markers CCR7 and CD206, macrophages on GG07-I showed an anti-inflammatory (M2) phenotype at 7 d. IL-4 mediates cytokine secretion, such as IL-10, TGF-β1, ARG-1, PDGF and VEGF, to inhibit the inflammatory response and promote angiogenesis by activating the Janus kinase-signal transducer and activator of transcription (JAK-STAT6) signalling pathway (Gordon *et al.*, 2010; Wang *et al.*, 2017). As IL-4 is released from GG07-I, the polarised M1 phenotype consequently transforms to the M2 phenotype, promoting the anti-inflammatory phase rather than

long-term dominance of inflammation. In the present study, inhibition of IL-1β, IL-6, and TNF-α and promotion of IL-10, TGF-β1, and ARG-1 in GG07-I macrophages at 5-7 d were observed. Moreover, IL-1β inhibits bone formation by suppressing BMP receptor expression and collagen synthesis (Chen *et al*., 2016). These secreted anti-inflammatory mediators enhance the healing ability of M2 macrophages. IL-10 inhibits the secretion of pro-inflammatory cytokines and NO (Mosser and Edwards 2008). ARG-1 converts arginine to ornithine, which prompts collagen synthesis and tissue remodelling (Sabanai *et al*., 2008). TGF-β1 is important for vessel stabilisation and maturation and can enhance chondrogenesis and neocartilage regeneration both *in vitro* and *in vivo* (Almubarak *et al*., 2016). Regarding angiogenesis, macrophages cultured on GG07-I exhibited increased VEGF secretion at 1-3 d and a higher PDGF-BB expression level at 7 d. In the process of blood vessel network growth, including sprouting, anastomosis and maturation of vessels, endothelial cells differentiate into tip cells and stalk cells in response to VEGF, which lead and support the sprouting vessels. Then, newly sprouted vessels fuse with other vessels and recruit pericytes using PDGF-BB to stabilise and develop the sprouts into mature vessels (Collier *et al*., 2004; Kalbacova *et al*., 2007). An efficient and timely switch from M1 macrophages with higher VEGF expression to M2 macrophages with higher PDGF-BB expression may result in stable and robust vessels.

In addition to cytokine release, structural and chemical cues provided by the biomaterials also affect immune responses and adjust cell behaviours temporally and spatially (Lu and Webster, 2015; Luu *et al*., 2015; Ma *et al*., 2014). The possible biological responses elicited by GG07 *in vitro* were explored. The macrophages on GG07 presented almost the same CD206 expression and IL-1β, IL-6, TNF-α, IL-10 and TGF-β1 secretion as those on PT. These results supported the notion that the IL-4 release contributed to a dominant role for M2 polarisation. Ideally, an implant should be able to induce both rapid osseointegration and angiogenesis. The results showed that GG07-I enhanced VEGF, PDGF-BB and BMP-2 expression simultaneously at 7 d. The synergistic action of PDGF-BB and BMP-2 induces excellent new bone regeneration (Del *et al*., 2015; Park *et al*., 2013). The combination of VEGF, PDGF-BB and BMP-2 has additive effects on elevation of the maxillary sinus and promotes cell differentiation during bone regeneration (Zhang *et al*., 2011; Chen *et al*., 2016). The findings reported here suggest that GG07-I might perform well *in vivo*. However, only studying macrophage polarisation is inadequate. Future research should focus on co-culture of macrophages with osteogenic cells and implantation *in vivo* to thoroughly analyse the modulatory effect of this biomaterial on macrophages.

## Conclusion

Cytokine IL-4-loaded titanium coatings with different extents of cross-linking were prepared using a sol-gel method. Release of the cytokine from the coatings was correlated with the extent of hydrogel cross-linking and the microenvironment. The hydrogel coating with a moderate extent of cross-linking (0.70 wt% genipin) allowed the greatest release of IL-4 from 3 d to 7 d and the lowest release within the first 3 d. This titanium coating modulated the temporal M1 to M2 polarisation of macrophages through delayed release of IL-4 in the simulated inflammatory microenvironment. The temporal shift from the M1 to M2 phenotype was confirmed at the cell, protein and gene levels and suggested a potential to promote vascularisation and osseointegration. Additionally, the method described here provided a reference for the design of biomaterials to modulate inflammation. Subsequent research will be performed to evaluate vascularisation and osseointegration *in vivo*.

## Acknowledgements

This work was supported by the National Natural Science Foundation of China (31570955), the National Key Research and Development Program of China (2017YFB0702602) and Foundation of Sichuan Normal University (SYJS2017010).

## References

Almubarak S, Nethercott H, Freeberg M, Beaudon C, Jha A, Jackson W, Marcucio R, Miclau T, Healy K, Bahney C (2016) Tissue engineering strategies for promoting vascularized bone regeneration. Bone **83**: 197-209.

Auger FA, Gibot L, Lacroix D (2013) The pivotal role of vascularisation in tissue engineering. Annu Rev Biomed Eng **15**: 177-200.

Babensee JE, Anderson JM, McIntire LV, Mikos AG (1998) Host response to tissue engineered devices. Adv Drug Deliv Rev **33**: 111-139.

Bigi A, Cojazzi G, Panzavolta S, Roveri N, Rubini K (2002) Stabilization of gelatin films by crosslinking with genipin. Biomaterials **23**: 4827-4832.

Brancato SK, Albina JE (2011) Wound macrophages as key regulators of repair: origin, phenotype, and function. Am J Pathol **178**: 19-25.

Brodbeck WG, Patel J, Voskerician G, Christenson E, Shive MS, Nakayama Y, Matsuda T, Ziats NP, Anderson JM (2002) Biomaterial adherent macrophage apoptosis is increased by hydrophilic and anionic substrates *in vivo*. Proc Natl Acad Sci U S A **99**: 10287-10292.

Brodbeck WG, Shive MS, Colton E, Nakayama Y, Matsuda T, Anderson JM (2001) Influence of

biomaterial surface chemistry on the apoptosis of adherent cells. J Biomed Mater Res Part A **55**: 661-668.

Carvalho V, Castanheira P, Faria TQ, Gonçalves C, Madureira P, Faro C (2010) Biological activity of heterologous murine interleukin-10 and preliminary studies on the use of a dextrin nanogel as a delivery system. Int J Pharm **400**: 234-242.

Chen YS, Chang JY, Cheng CY, Tsai FJ, Yao CH, Liu BS (2005) An *in vivo* evaluation of a biodegradable genipin-cross-linked gelatin peripheral nerve guide conduit material. Biomaterials **26**: 3911-3918.

Chen ZT, Klein T, Murray RZ, Crawford R, Chang J, Wu CT, Xiao Y (2016) Osteoimmunomodulation for the development of advanced bone biomaterials. Materials Today **19**: 304-321.

Collier TO, Anderson JM, Brodbeck WG, Barber T, Healy KE (2004) Inhibition of macrophage development and foreign body giant cell formation by hydrophilic interpenetrating polymer network. J Biomed Mater Res Part A **69**: 644-650.

Conway EM, Collen D, Carmeliet P (2001) Molecular mechanisms of blood vessel growth. Cardiovasc Res **49**: 507-521.

Daley JM, Brancato SK, Thomay AA, Reichner JS, Albina JE (2010) The phenotype of murine wound macrophages. J Leukocyte Biol **87**: 59-67.

Del RC, Rodriguez-Evora M, Reyes R, Delgado A, Evora C (2015) BMP-2, PDGF-BB, and bone marrow mesenchymal cells in a macroporous β-TCP scaffold for critical-size bone defect repair in rats. Biomed Mater **10**: 045008.

Epelman S, Lavine KJ, Randolph GJ (2014) Origin and functions of tissue macrophages. Immunity **41**: 21-35.

Fakhry A, Schneider G.B, Zaharias R, Senel S (2004) Chitosan supports the initial attachment and spreading of osteoblasts preferentially over fibroblasts. Biomaterials **25**: 2075-2079.

Forbes SJ, Rosenthal N (2014) Preparing the ground for tissue regeneration: from mechanism to therapy. Nat Med **20**: 857-869.

Fujisaka S, Usui I, Bukhari A, Ikutani M, Oya T, Kanatani Y, Tsuneyama K, Nagai Y, Takatsu K, Urakaze M (2009) Regulatory mechanisms for adipose tissue M1 and M2 macrophages in diet-induced obese mice. Diabetes **58**: 2574-2582.

Gordon S, Martinez FO (2010) Alternative activation of macrophages: mechanism and functions. Immunity **32**: 593-604.

Grayson WL, Frohlich M, Yeager K, Bhumiratana S, Chan ME, Cannizzaro C (2010) Engineering anatomically shaped human bone grafts. Proc Natl Acad Sci U S A **107**: 3299-3304.

Hellberg C, Ostman A, Heldin CH (2010) PDGF and vessel maturation. Recent Results Cancer Res **180**: 103-114.

Hotamisligil GS (2006) Inflammation and metabolic disorders. Nature **444**: 860-867.

Kalbacova M, Roessler S, Hempel U, Tsaryk R, Peters K, Scharnweber D, Kirkpatrick JC, Dieter P (2007) The effect of electrochemically simulated titanium cathodic corrosion products on ROS production and metabolic activity of osteoblasts and monocytes/macrophages. Biomaterials **28**: 3263-3272.

Kanczler JM, Oreffo RO (2008) Osteogenesis and angiogenesis: the potential for engineering bone. Eur Cell Mater **15**: 100-114.

Koh TJ, DiPietro LA (2011) Inflammation and wound healing: the role of the macrophage. Expert Rev Mol Med **13**: 11-23.

Koo HJ, Lim KH, Jung HJ, Park EH (2006) Anti-inflammatory evaluation of gardenia extract, geniposide and genipin. J Ethnopharmacol **103**: 496-500.

Koo HJ, Song YS, Kim HJ, Lee YH, Hong SM, Kim SJ, Kim BC, Jin C, Lim CJ, Park EH (2004) Anti-inflammatory effects of genipin, an active principle of gardenia. Eur J Pharmacol **495**: 201-208.

Lai JY (2013) Corneal stromal cell growth on gelatin/chondroitin sulfate scaffolds modified at different NHS/EDC molar ratios. Int J Mol Sci **14**: 2036-2055.

Laschke MW, Kleer S, Scheuer C, Schuler S, Garcia P, Eglin D, Alini M, Menger MD (2012) Vascularisation of porous scaffolds is improved by incorporation of adipose tissue-derived microvascular fragments. Eur Cell Mater **24**: 266-277.

Lauer G, Sollberg S, Cole M, Flamme I, Sturzebecher J, Mann K, Krieg T, A.Eming S (2000) Expression and proteolysis of vascular endothelial growth factor is increased in chronic wounds. J Invest Dermatol **115**: 12-18.

Lien SM, Li WT, Huang TJ (2008) Genipin-crosslinked gelatin scaffolds for articular cartilage tissue engineering with a novel crosslinking method. Mater Sci Eng C **28**: 36-43.

LogithKumar A, KeshavNarayan A, Dhivya S, Chawla A, Saravanan S, Selvamurugan N (2016) A review of chitosan and its derivatives in bone tissue engineering. Carbohydr Polym **151**: 172-188.

Lu J, Webster TJ (2015) Reduced immune cell responses on nano and submicron rough titanium. Acta Biomater **16**: 223-231.

Luttikhuizen DT, van Amerongen MJ, de Feijter PC, Petersen AH, Harmsen MC, van Luyn MJ (2006) The correlation between difference in foreign body reaction between implant locations and cytokine and MMP expression. Biomaterials **27**: 5763-5770.

Luu TU, Gott SC, Woo BW, Rao MP, Liu WF (2015) Micro- and nanopatterned topographical cues for regulating macrophage cell shape and phenotype. ACS Appl Mater Interfaces **7**: 28665-28672.

Ma QL, Zhao LZ, Liu RR, Jin BQ, Song W, Wang Y, Zhang YS, Chen LH, Zhang YM (2014) Improved implant osseointegration of a nanostructured titanium surface *via* mediation of macrophage polarization. Biomaterials **35**: 9853-9867.

MacLauchlan S, Skokos EA, Meznarich N, Zhu DH, Raoof S, Shipley JM (2009) Macrophage fusion, giant cell formation, and the foreign body response require matrix metalloproteinase 9. J Leukocyte Biol **85**: 617-626.

Madden LR, Mortisen DJ, Sussman EM, Dupras SK, Fugate JA, Cuy JL (2010) Proangiogenic scaffolds as functional templates for cardiac tissue engineering. Proc. Proc Natl Acad Sci U S A **107**: 15211-15216.

Martinez FO, Gordon S (2014) The M1 and M2 paradigm of macrophage activation: time for reassessment. F1000Prime Rep **6**: 13.

Martinez FO, Gordon S, Locati M, Mantovani A (2006) Transcriptional profiling of the human monocyte-to-macrophage differentiation and polarization: new molecules and patterns of gene expression. J Immunol **177**: 7303-7311.

Mi FL, Sung HW, Shyu SS (2000) Synthesis and characterization of a novel chitosan-based network prepared using naturally occurring crosslinker. J Polym Sci A Polym Chem **38**: 2804-2814.

Mosser DM, Edwards JP (2008) Exploring the full spectrum of macrophage activation. Nat Rev Immunol **8**: 958-969.

Mountziaris PM, Mikos AG (2008) Modulation of the inflammatory response for enhanced bone tissue regeneration. Tissue Eng Part B Rev **14**: 179-186.

Murray PJ, Allen JE, Biswas SK, Fisher EA, Gilroy DW, Goerdt S, Gordon S, Hamilton JA, Ivashkiv LB, Lawrence T (2014) Macrophage activation and polarization: nomenclature and experimental guidelines. Immunity **41**: 14-20.

Nickerson MT, Patel J, Heyd D V, Rousseau D, Paulson AT (2006) Kinetic and mechanistic considerations in the gelation of genipin-crosslinked gelatin. Int J Biol Macromol **39**: 2983-2302.

Novosel EC, Kleinhans C, Kluger PJ (2011) Vascularisation is the key challenge in tissue engineering. Adv Drug Deliv Rev **63**: 300-311.

Park SY, Kim KH, Shin SY, Koo KT, Lee YM, Seol YJ (2013) Dual delivery of rhPDGF-BB and bone marrow mesenchymal stromal cells expressing the BMP2 gene enhance bone formation in a critical-sized defect model. Tissue Eng Part A **19**: 2495-2505.

Reeves ARD, Spiller KL, Freytes DO, Vunjak-Novakovic G, Kaplan DL (2015) Controlled release of cytokines using silk-biomaterials for macrophage polarization. Biomaterials **73**: 272-283.

Roh JD, Sawh-Martinez R, Brennan MP, Jay SM, Devine L, Rao DA (2010) Tissue engineered vascular grafts transform into mature blood vessels *via* an inflammation-mediated process of vascular remodeling. Proc Natl Acad Sci U S A **107**: 4669-4674.

Sabanai K, Tsutsui M, Sakai A, Hirasawa H, Tanaka S, Nakamura E, Tanimoto A, Sasaguri Y, Ito M, Shimokawa H (2008) Genetic disruption of all NO synthase isoforms enhances BMD and bone turnover in mice *in vivo*: involvement of the renin-angiotensin system J Bone Miner Res **23**: 633-643.

Santoro M, Tatara AM, Mikos AG (2014) Gelatin carriers for drug and cell delivery in tissue engineering. J Control Release **190**: 210-218.

Spiller KL, Anfang RR, Spiller KJ, Ng J, Nakazawa KR, Daulton JW (2014) The role of macrophage phenotype in vascularization of tissue engineering scaffolds. Biomaterials **35**: 4477-4488.

Spiller KL, Nassiri S, Witherel CE, Anfang RR, Ng J, Nakazawa K R, Yu T, Vunjak-Novakovic G (2015) Sequential delivery of immunomodulatory cytokines to facilitate the M1-to-M2 transition of macrophages and enhance vascularization of bone scaffolds. Biomaterials **37**: 194-207.

Sun YH, Li YT, Wu BH, Wang JX, Lu X, Qu SX, Weng J, Feng B (2017) Biological responses to M13 bacteriophage modified titanium surfaces *in vitro*. Acta Biomater **58**: 527-538.

Takemura R, Werb Z (1984) Secretory products of macrophages and their physiological functions. Am J Physiol **246**: C1-C9.

Tarnuzzer RW, Schultz GS (1996) Biochemical analysis of acute and chronic wound environments. Wound Rep Reg **4**: 321-325.

Wang J, Qian S, Liu XY, Xu LY, Miao XC, Xu ZY, Cao LY, Wang HL, Jiang XQ (2017) M2 macrophages contribute to osteogenesis and angiogenesis on nanotubular $TiO_2$ surfaces. J Mater Chem B **5**: 3364-3376.

Yager DR, Chen SM, Ward SI, Olutoye OO. Diegelmann RF, Cohen IK (1997) Ability of chronic wound fluids to degrade peptide growth factors is associated with increased levels of elastase activity and diminished levels of proteinase inhibitors. Wound Rep Reg **5**: 23-32.

Yancopoulos GD, Davis S, Gale NW, Rudge JS, Wiegand SJ, Holash J (2000) Vascular specific growth factors and blood vessel formation. Nature **407**: 242-248.

Yao CH, Liu BS, Chang CJ, Hsu SH, Chen YS (2004) Preparation of networks of gelatin and genipin as degradable biomaterials. Mater Chem Phys **83**: 204-208.

Yeoh-Ellerton S, Stacey MC (2003) Iron and 8-isoprostane levels in acute and chronic wounds. J Invest Dermatol **121**: 918-925.

Yin J, Ferguson TA (2009) Identification of an IFN-gamma-producing neutrophil early in the response to *Listeria* monocytogenes. J Immunol **182**: 7069-7073.

Young S, Wong M, Tabata Y, Mikos AG (2005) Gelatin as a delivery vehicle for the controlled release of bioactive molecules. J Control Release **109**: 256-274.

Zhang W, Wang X, Wang S, Zhao J, Xu L, Zhu C, Zeng D, Chen J, Zhang Z, Kaplan DL (2011) The use of injectable sonication-induced silk hydrogel for VEGF and BMP-2 delivery for elevation of the maxillary sinus floor. Biomaterials **32**: 9415-9424.

## Discussion with reviewers

**Yvonne Bastiaansen-Jenniskens**: The authors describe a culture model in which macrophages were cultured on the surface of the material. After 7 d of culture, the number of cells seemed to decrease, the morphology of the cells changed, and as the authors report, the macrophages seemed to have altered the surface of the material. Can the authors speculate on how this would translate to the *in vivo* situation,

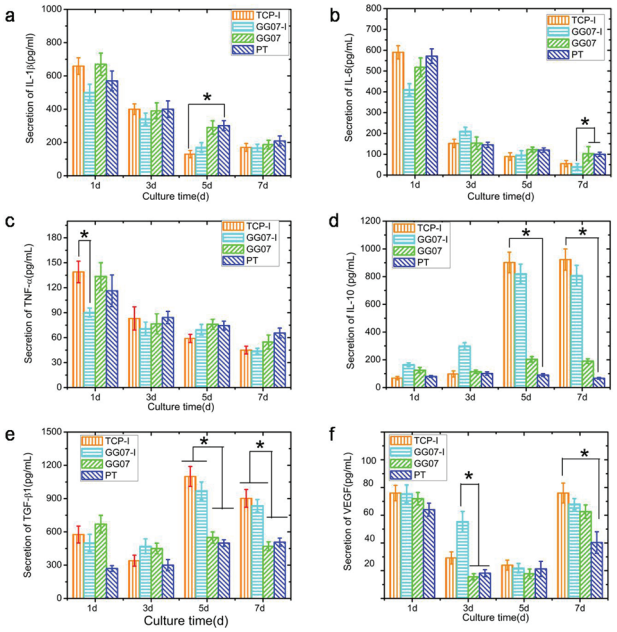


**Fig. 11. Cytokine and growth factor secretion**. Secreted levels of (**a**) IL-1β, (**b**) TNF-α, (**c**) IL-6, (**d**) VEGF, (**e**) IL-10 and (**f**) TGF-β1 in the supernatants of macrophages cultured on different surfaces for 1, 3, 5 and 7 d. $n = 3$, * $p < 0.05$.

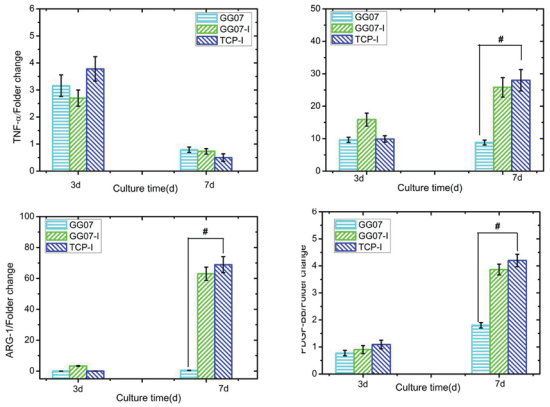


**Fig. 12. Cytokine and growth factor gene expression**. Gene expression of (**a**) TNF-α, (**b**) IL-10, (**c**) ARG-1 and (**d**) PDGF-BB analysed by RT-PCR after 3 and 7 d of culture. $n = 3$, # $p < 0.05$.

especially regarding decrease of cell numbers and altered cell morphology?

I guess the material is then still able to influence macrophage phenotype of cells surrounding the material but not necessarily attached to the material (assuming they don't reduce in cell number and change morphology because they are dying). Would an experiment in which cells are not adhering to the material but are present in the same well as the material also be relevant to perform?

**Authors**: Acute inflammation occurs at an implant site just after the deposition of fibrinogen and blood clotting. Neutrophil infiltration monocytes are recruited to the implant, differentiate into inflammatory macrophages within the first 24 h. These M1 macrophages adhere to the biomaterial, spread on its surface, defend against bacterial infections, phagocytose dead cells, and stimulate blood vessel sprout. The gelatine coating was beneficial to initial macrophage adhesion and viability within the first 5 d *in vitro*. I guess GG07-I and GG07 prompted initial wound clean and blood vessel sprout *in vivo* in contrast with PT. The morphology of macrophages on GG07-I at 5 d changed to spindle-shaped, due to IL-4 stimulation. The adherent cell density reached a peak at 5 d and then decreased at 7 d. In addition, FBGCs were not observed on biomaterials in the culture up to 7 d. In the later stage (5-7 d), GG07-I showed higher expression of IL-10 and PDGF-BB. These soluble molecules activate keratinocytes, fibroblasts and osteoblasts, indicating an emergence of inflammation regression and successful healing. Based on experiment *in vitro*, we speculated that these delivery devices would achieve improved healing *in vivo* (initial stage: phagocytosis of dead cells, new blood vessel sprout, later stage: no capsule or greatly reduced capsule formation). The comparison between loading cytokines into the material system and adding into culture media directly was necessary. Because the real amount of IL-4 in the cultural process is hard to quantify, we chose 20 ng/mL IL-4 (based on release profile). Cells cultured on TCP with culture media were supplemented by IFN-γ at the first 3 d and replaced with IL-4 (20 ng/mL). They were denoted as TCP-I. According to the results of ELISA and PCR, the expression levels of the related cytokines were very similar to that of GG07-I (Fig.11, Fig.12). All these data indicated that biomaterials had no apparent effect on macrophage polarisation compared with the IL-4.

**Editor's note**: The Scientific Editor responsible for this paper was Martin Stoddart.